

UPPSALA UNIVERSITY
INSTITUTE OF PHYSICS



SID 3 SAKNAS

Measurements of $B(E2, 0^+ \rightarrow 2^+)$ for
even Xe isotopes

L.-O. Edvardson and L.-O. Norlin
Uppsala University, Institute of Physics
Box 530, S-751 21 Uppsala, Sweden

UIIP-869

April 1974

Abstract: Transition moments and lifetimes have been deduced from measurements of the Coulomb excitation cross sections for $^{128,130,132,134,136}\text{Xe}$ isotopes. The results are for $B(E2)$ [0.77(6); 0.60(6); 0.49(4); 0.38(6); 0.17(3)] $e^2 \times 10^{-48} \text{ cm}^4$ and for $\tau(2^+)$ [31.6(24); 15.3(15); 6.3(6); 2.4(4); 0.59(15)] psec going from ^{128}Xe to ^{136}Xe .

1. Introduction

Both microscopic and collective calculations have been made in the mass region with $50 < (N,Z) < 82$ [1 - 4]. Nuclear quantities like $B(E2)$, Q_0 and g are the most important probes for testing nuclear models and for classifying nuclei. Here are reported measurements of Coulomb excitation cross sections for five even Xe nuclei. From the cross sections $B(E2 0^+ \rightarrow 2_1^+)$ and $\tau(2_1^+)$ was deduced. During the last years the use of surface barrier detectors has improved the measurements of excitation cross sections considerably. Using these detectors the inelastically scattered particles can be resolved from the elastic ones. Good accuracy and reproducibility is obtained. The present measurements on Xe were made possible since a new technique for collection of large amounts of xenon in solid targets has been developed at this institute [5].

2. General remarks

Measurements of absolute Coulomb excitation cross sections (σ_c) are in general difficult to perform. Energy integral detection of backscattered particles makes it possible to relate the excitation cross section to the wellknown Rutherford scattering cross section:

$$d\sigma_R = \frac{1}{4} \frac{a^2}{\sin^4\left(\frac{\theta}{2}\right)} d\Omega$$

where $2a$ is the distance of closest approach.

By comparing the number of inelastically scattered particles to those scattered elastically σ_c can be deduced.

In order to extract σ_{2^+} from experimentally determined relative intensities only corrections for transformation from CM - to Lab. system has to be applied. In first order σ_{2^+} is proportional to $B(E2)$. The so called reorientation

effect contributes to σ_{2+} in proportion to the quadrupole moment of the excited state. Virtual excitations of higher lying levels interfere constructively or destructively resulting in corrections to σ_{2+} . When deriving $B(E2)$ from σ_{2+} these effects have to be considered.

3. Experimental technique

In spite of the moderate energy resolution of surface barrier detectors (compared to magnetic spectrometers) for α particles and heavy ions it is usually possible to resolve the inelastic peak from the elastic. The efficiency is independent of energy and can be assumed equal to unity if the peripheral regions are masked off. The experiments were performed in the 38 cm radius charged particle scattering chamber [18].

An annular surface barrier detector (300 mm^2) was used in a backscatter geometry with the average scattering angle either 175° or 178° . The experiments were performed with α beams of energies 11-13 MeV collimated to 3 mm^2 . The solid angle was kept well below the limit where kinematic broadening becomes noticeable. The system resolution as measured with an ^{226}Ra α -emitting source was $\sim 30 \text{ keV}$ (FWHM).

The ions loose energy in the target layer and therefore the targets have to be kept quite thin. In the present measurements Xe thicknesses of $25\text{-}90 \text{ }\mu\text{g}/\text{cm}^2$ were used. The targets were prepared by implantation into a carbon layer on an iron backing. The method in which an isotopic separator is used is described in reference [5]. The targets were originally prepared for IMPAC-experiments and therefore the iron backings were quite thick ($\sim 0.1 \text{ mm}$). The effects mentioned above resulted in an overall α particle resolution of $\sim 100 \text{ keV}$ (FWHM). The mean energy of the ion at the moment of impact was estimated to be $\sim 25 \text{ keV}$ lower than the beam energy. However the major advantage with implanted targets is their extreme purity.

In Fig. 1 the spectrum from 13 MeV α -scattering is shown.



5. Test measurements on ^{128}Te

A measurement on ^{128}Te was performed in order to check the reliability of this type of measurements. In table I the present results are compared to published data [13,16]. In the analysis of the present ^{128}Te data Q_{2+} was set equal to the mean of Q_{2+} obtained from these two measurements. The present result for $B(E2)$ agrees well with that of Kleinfeld et al. but not so well with the results of Stokstad and Hall. Kleinfeld et al. measured the particle scattering cross section whereas Stokstad and Hall observed coincidences between scattered particles and gammas. Kleinfeld states that for ^{128}Te deviations from pure electromagnetic excitation occurred at energies above 10.5 MeV. The measurement at 12 MeV gives the lowest value of $B(E2)$, which might indicate presence of a small destructive interference from direct nuclear excitation. For the 12 MeV experiments on Xe the interference from nuclear excitation is less due to the higher Coulomb barrier. Cline [17] has suggested for the highest safe bombarding energy

$$E_B = 1.44 \left(1 + \frac{A_1}{A_2} \right) \frac{Z_1 Z_2}{1.25 \left(A_1^{1/3} + A_2^{1/3} \right) + 5.1} \text{ (MeV)}$$

For α -bombardment of ^{130}Xe one obtains 11.9 MeV. Christy and Häusser accepted measurements which were performed up to 10% above E_B in their compilation of quadrupole moments [14].

Discussion

Fig. 4 shows a plot of the energies of the first $2+$ level for all known Xe isotopes. In Fig. 3 and table II the results of the present experiments are given. A strong increase in $B(E2)$ is seen when the neutron number decreases. This is of course expected as the neutron deficient Xe isotopes are close to a region where nuclear deformation is possible [4]. Compared to the Weisskopf estimate, the E2-enhancement varies from ~ 10 for ^{136}Xe to ~ 40 for ^{128}Xe . As can be seen from Fig. 3 the experimental trend for the $B(E2)$'s is nicely reproduced by the theoretical calculations of ref. [1] and [3]. The magnitudes

are well fitted if $e_{\text{eff}} = 0.2$ is used in the theory of Uher and Sorensen [1]. The values of Habs et al. [3] are all consistently somewhat too small. The rather large errors in the $B(E2)$ values come from the uncertainties in the analysis. As mentioned in section 4 a non-vanishing static quadrupole moment gives an appreciable contribution to the excitation cross section. For example: if the Q_{2+} changes from +0.4 eb to -0.4 eb, the deduced $B(E2, 0^+ \rightarrow 2^+)$ will decrease about 6% for ^{128}Xe . Neither of these quadrupole moment can be regarded as unrealistic. These uncertainties would be greater if heavier ions than α were used. Measurements of Q_{2+} must, conclusively, be made to get higher accuracy for the $B(E2)$ -values in the Xe isotopes.

Acknowledgements

Drs A. Arnesen and T. Noreland are heartily thanked for their big efforts to produce these unic targets. We are deeply indebted to Dr B. Sundqvist for putting his equipment to our disposal and teaching us how to use it. The staff of the Uppsala Tandem accelerator laboratory is thanked for their assistance.

References

1. R.A. Uher and R.A. Sorensen, Nucl. Phys. 86 (1966) 1.
2. L.S. Kisslinger and R.A. Sorensen, Rev. Mod. Phys. 35 (1963) 853.
3. D. Habs, H. Klewe-Nebenius, K. Wisshak, R. Löhken, G. Nowicki and H. Rebel, Z. Physik 267 (1974) 149.
4. D.A. Arseniev, A. Sobiczewski and V.G. Soloviev, Nucl. Phys. A126 (1969) 15.
5. A. Arnesen, T. Noreland and L.-O. Norlin, Uppsala University, Institute of Physics, UUIP-870 (April 1974).
6. W. Kutschera, W. Dehnhardt, O.C. Kistner, P. Kump, P. Bovh and H.J. Sann, Physical Review C 5 (1972) 1658.
7. D. Gordon, L. Eytel, H. de Waard, E.N. Kaufmann and D. Murnick, Proceedings of the Int. Conf. on Nuclear Physics, (eds. J. de Boer and H.J. Mang), North Holland Publ. Co., Amsterdam (1973) p. 259.
8. T.J. de Boer, E.W. Ten Napel and J. Blok, Physica 29 (1963) 1013.
9. P.F. Kenealy, G.B. Beard and K. Parsons, Physical Review C 2 (1970) 2009.
10. G.F. Pieper, C.E. Anderson and N.P. Heydenberg, Bull. Am. Phys. Soc. 3 (1958) 38.
11. W.D. Hamilton, Proc. Phys. Soc. (London) 78 (1961) 1064.
12. A. Winther and J. de Boer in Coulomb Excitation (eds. K. Alder and A. Winther) Academic Press, New York, 1966 p. 303.
13. R.G. Stokstad and I. Hall, Nucl. Phys. 99 (1967) 507.
14. A. Christy and O. Häusser, Nuclear Data Tables 11 (1972) 281.
15. S. Sen, P.J. Riley and T. Udagava, Phys. Rev. C 6 (1972) 2201.
16. A.M. Kleinfeld, G. Maggi and W. Werdecker, Proc. of the Int. Conf. on Nuclear Moments and Nuclear Structure 1972. (eds. H. Horie and K. Sugimoto). Journ. Phys. Soc. Jap. 34 (1973) 440.

17. D. Cline, P. Jennens, C.W. Towsley and H.S. Gertzman,
Bull. Am. Phys. Soc. 16 (1971) 1156.
18. S. Pettersson and B. Sundqvist, Uppsala University,
Institute of Technology UPTEC 73 27R (May 1973).

Table captions

Table I. Results of experiments and analysis.

* For ^{128}Te , the upper value of Q (in each row) is obtained if constructive interference is assumed.

Table II. Summary of experimental and theoretical results for $B(E2)$ and Q_{2+} of even Xenon isotopes.

The formula (or its inverse)

$$B(E2, 0^+ \rightarrow 2^+) = \frac{4.08 \cdot 10^{-13}}{[E_{2+}(\text{MeV})]^5 \cdot \tau(\text{s}) \cdot (1+\alpha)} (e^2 b^2)$$

was used.

The shorthand notations for the different experimental methods are as follows:

γLS τ obtained from lineshape analysis of dopplershifted γ lines.

NRF Nuclear resonance fluorescence.
Level width determined.

$^{16}\text{O}\gamma$ Excitation cross section determined from rate of coincidences between backscattered ^{16}O ions and deexcitation gammas.

$\sigma(\theta_\alpha)$ Excitation cross section from spectrum of backscattered alpha particles.

*From reference 1 $B(E2)$ for $e_{\text{eff}} = 0.2$ was chosen.

**From reference 4 Q_{2+} corresponding to the most favourable deformation energy was chosen.

Figure captions

- Fig. 1: σ_c/σ_R versus M_{12} for two different Q_{2+} -values for ^{128}Xe .
- Fig. 2: Spectrum of 13 MeV α particles backscattered from ^{136}Xe on iron.
- Fig. 3: Present experimental results compared to theoretical estimates.
- Fig. 4: E_{2+} for Xe isotopes.

Table I

ANALYSIS

A	$E(2^+)$ (keV)	E_{α} (MeV)	$\frac{\text{Inelastic}}{\text{Elastic}}$ (%)	$ Q_{2^+} ^{\text{Max}}$ (*)	$B(E2; 0^+ \rightarrow 2^+)$ $e^+ \times 10^{-48} \text{ cm}^4$	Reference
^{128}Xe	442.9	11.0	1.49(21)	0.76	0.82(13)	This work
"	"	12.0	1.94(9)	"	0.76(6)	"-
^{130}Xe	538.0	12.0	1.33(9)	0.76	0.60(6)	"-
^{132}Xe	667.8	12.0	0.88(4)	0.76	0.49(4)	"-
^{134}Xe	854.0	12.0	0.51(7)	0.38	0.38(6)	"-
^{136}Xe	1313.3	13.0	0.147(22)	0.38	0.17(3)	"-
^{128}Te	743.2	11.0	0.48(6)	-	0.38(4)	"-
"	"	12.0	0.670(24)	-	0.354(12)	"-
"	"	≤ 10.5		-0.27(13) or -0.11(10)	0.389(5)	[13]
"	"	≤ 10.6		-0.07(9) or +0.12(9)	0.370(5)	[16]

Table II

A	N	E(2+) (keV)	B(E2) $e^2 \times 10^{-48} \text{cm}^4$	τ (ps)	Method	B(E2) theory		Q(2+) theory		Reference
						ref.1*	ref.3	ref.3	ref.4**	
120	66	321.8	1.84(22)	124(15)	γ LS				+0.86	6
122	68	331.5	2.21(20)	89(8)	γ LS				+0.80	6
124	70	354.1	0.84(7)	84(7)	$^{16}\text{O}\gamma$				+0.77	7
126	72	388.5	0.76(3)	59.6(20)	TM	0.788	0.45	-0.13	+0.63	8
			0.78(6)	59(5)	$^{16}\text{O}\gamma$					7
128	74	442.9	0.66(5)	37(3)	$^{16}\text{O}\gamma$	0.644	0.39	-0.29		7
			0.96	13(3)	NRF/ $^{16}\text{O}\gamma$					9,10
			0.77(6)	31.6(24)	$\sigma(\theta_\alpha)$					present
130	76	538.0	0.69(15)	13.3(24)	NRF	0.564	0.29	-0.05		9
			1.00(8)	9.2(8)	$^{16}\text{O}\gamma$					7
			0.60(6)	15.3(15)	$\sigma(\theta_\alpha)$					present
132	78	667.8	0.30(14)	9.7(30)	NRF	0.448	0.18	-0.01		11
			0.45	6.8	NRF/ $^{16}\text{O}\gamma$					9,10
			0.42(3)	7.3(6)	$^{16}\text{O}\gamma$					7
			0.49(4)	6.3(6)	$\sigma(\theta_\alpha)$					present
134	80	(854)	0.38(6)	2.4(4)	$\sigma(\theta_\alpha)$	0.370	0.12	+0.13		present
136	82	1313.3	0.17(3)	0.59(15)	$\sigma(\theta_\alpha)$	0.254				present

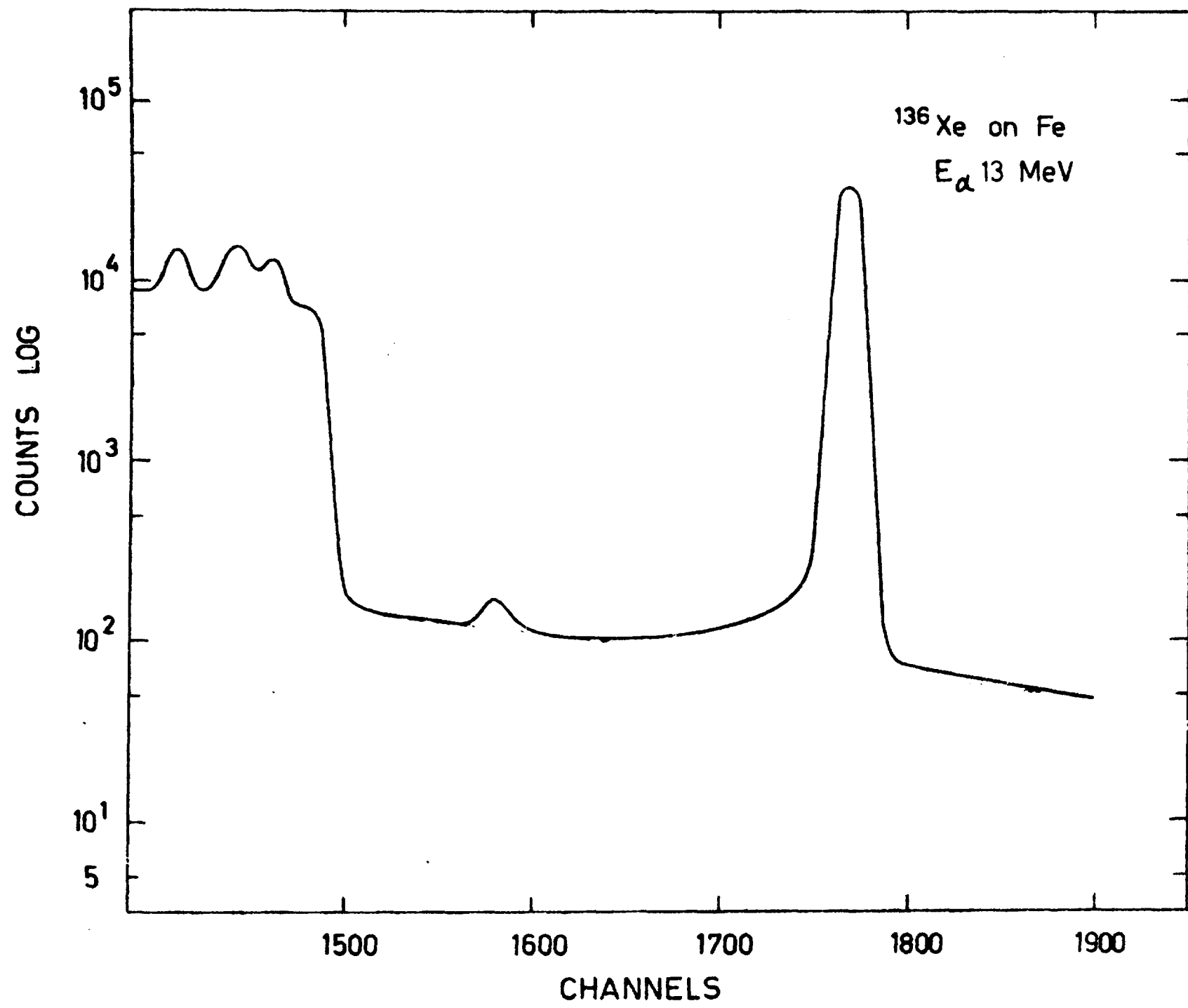


FIG. 1

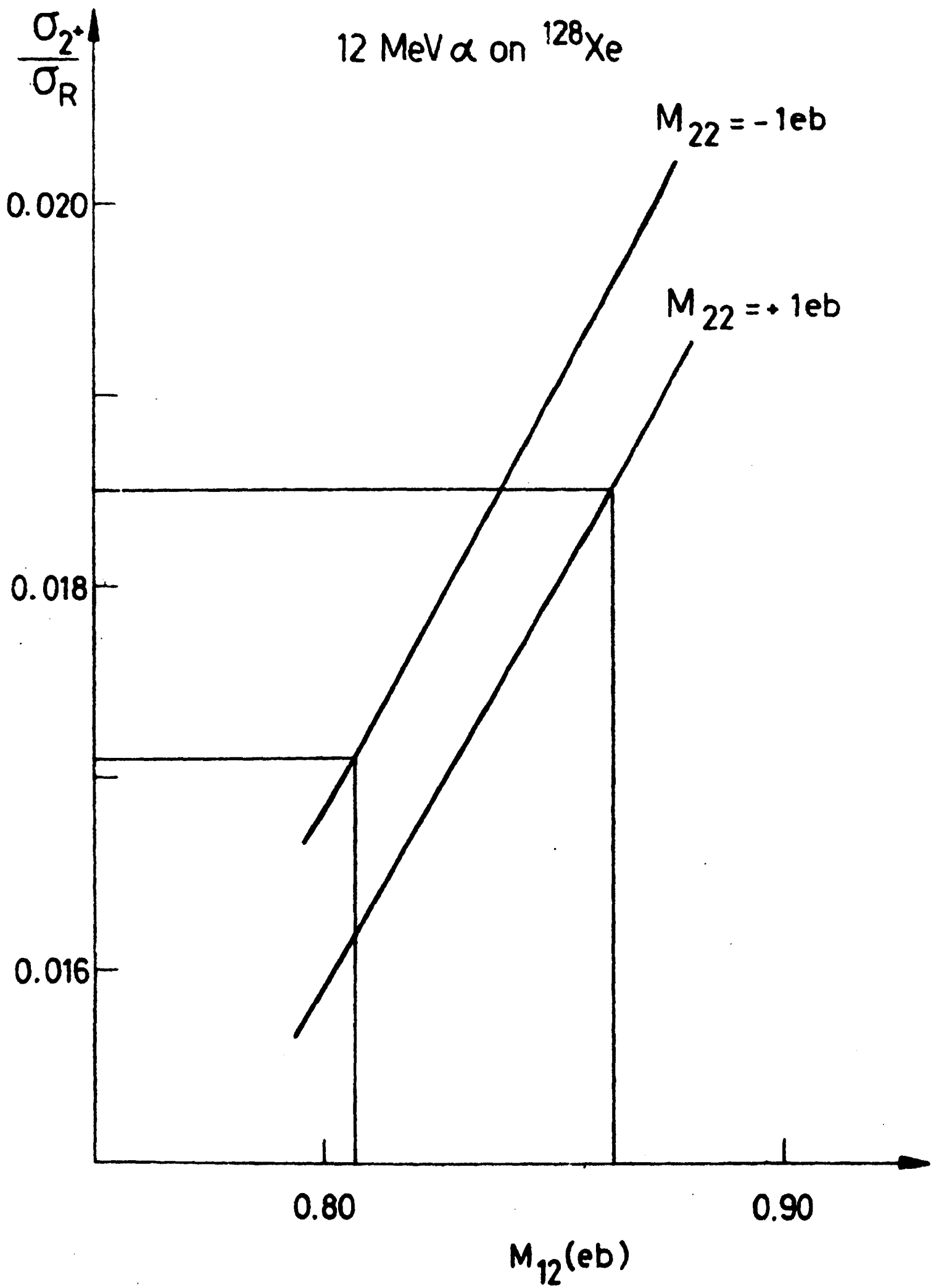


FIG. 2

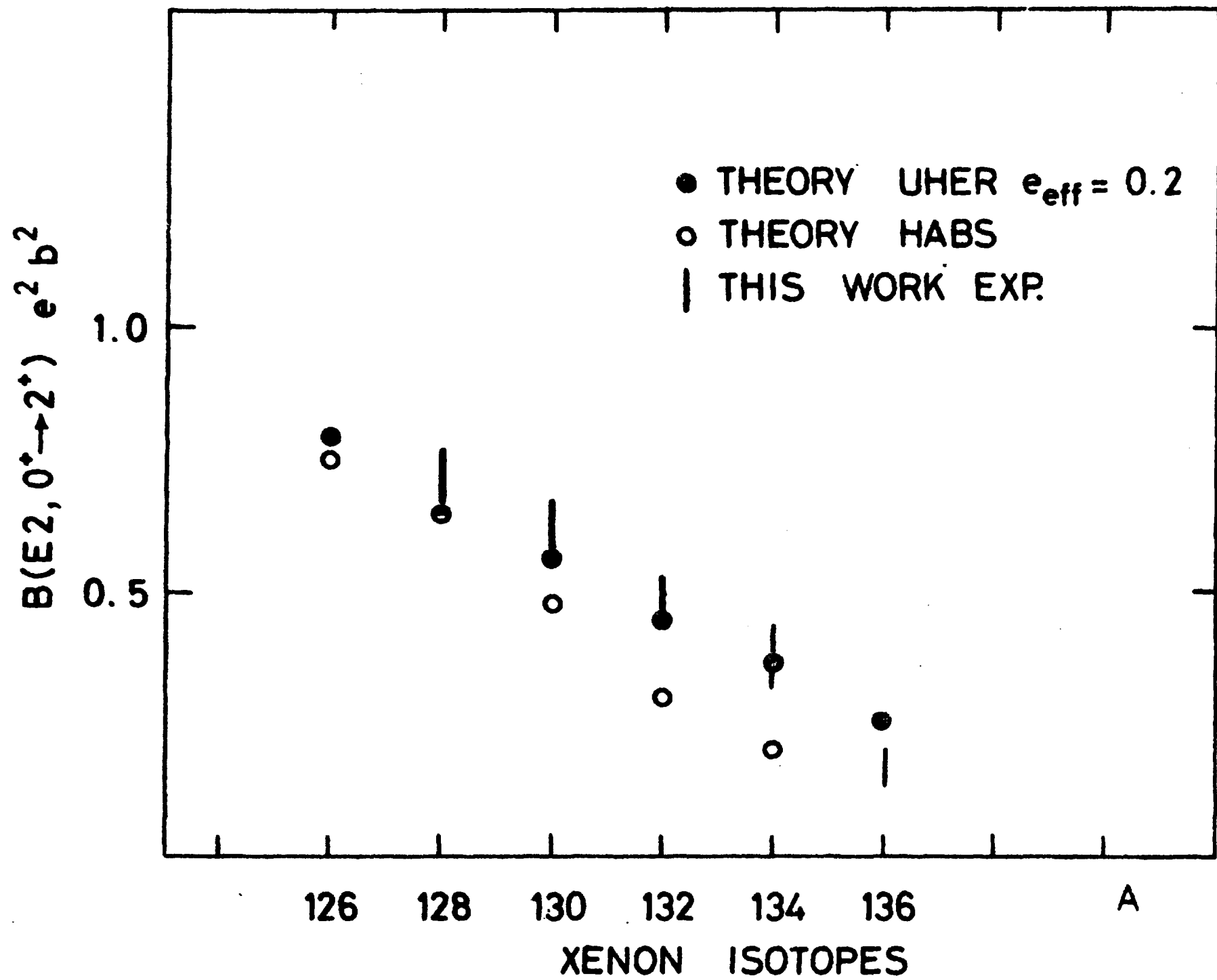


FIG. 3

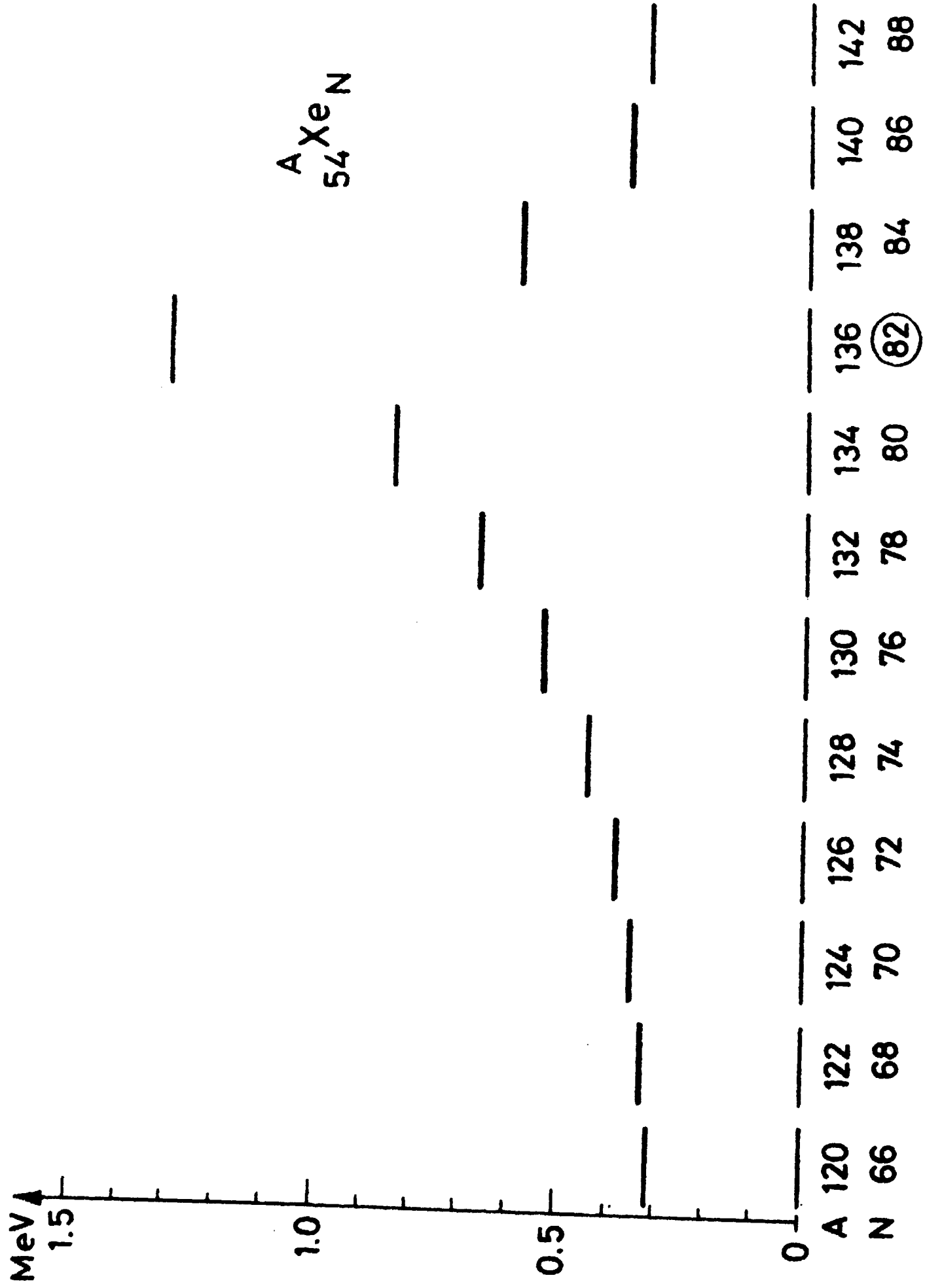


FIG. 4